2-2019

Extending the Osmometer Method for Assessing Drought Tolerance in Herbaceous Species

Robert J. Griffin-Nolan
Colorado State University

Troy W. Ocheltree
Colorado State University

Kevin E. Mueller
Cleveland State University, k.mueller89@csuohio.edu

Dana M. Blumenthal
USDA Agricultural Research Service

Julie A. Kray
USDA Agricultural Research Service

Recommended Citation

Authors

Robert J. Griffin-Nolan, Troy W. Ocheltree, Kevin E. Mueller, Dana M. Blumenthal, Julie A. Kray, and Alan K. Knapp

Extending the osmometer method for assessing drought tolerance in herbaceous species

Robert J. Griffin-Nolan[1,2] · Troy W. Ocheltree[2,3] · Kevin E. Mueller[4] · Dana M. Blumenthal[5] · Julie A. Kray[5] · Alan K. Knapp[1,2]

Abstract

Community-scale surveys of plant drought tolerance are essential for understanding semi-arid ecosystems and community responses to climate change. Thus, there is a need for an accurate and rapid methodology for assessing drought tolerance strategies across plant functional types. The osmometer method for predicting leaf osmotic potential at full turgor (π_o), a key metric of leaf-level drought tolerance, has resulted in a 50-fold increase in the measurement speed of this trait; however, the applicability of this method has only been tested in woody species and crops. Here, we assess the osmometer method for use in herbaceous grassland species and test whether π_o is an appropriate plant trait for understanding drought strategies of herbaceous species as well as species distributions along climate gradients. Our model for predicting leaf turgor loss point (π_{TLP}) from π_o ($\pi_{TLP} = 0.80\pi_o - 0.845$) is nearly identical to the model previously presented for woody species. Additionally, π_o was highly correlated with π_{TLP} for graminoid species ($\pi_{tlp} = 0.944\pi_o - 0.611$; $r^2 = 0.96$), a plant functional group previously flagged for having the potential to cause erroneous measurements when using an osmometer. We report that π_o, measured with an osmometer, is well correlated with other traits linked to drought tolerance (namely, leaf dry matter content and leaf vulnerability to hydraulic failure) as well as climate extremes linked to water availability. The validation of the osmometer method in an herb-dominated ecosystem paves the way for rapid community-scale surveys of drought tolerance across plant functional groups, which could improve trait-based predictions of ecosystem responses to climate change.

Keywords Osmotic potential · Climate change · Grasslands · Plant traits · Drought

Introduction

Accurate and efficient quantification of drought tolerance within plant communities is needed given that water is a primary limiting resource for plants across much of the world (Knapp et al. 2017) and extreme droughts are expected to become more common with climate change (Dai 2011; 2013; IPCC 2013). The response of ecosystem processes, such as aboveground net primary productivity, to drought has been shown to vary among ecosystems (Huxman et al. 2004), even within the same biome (Knapp et al. 2015); however, a mechanistic understanding of this variability is lacking. Hydraulic traits, such as leaf turgor loss point and xylem vulnerability to cavitation, can provide a mechanistic understanding of plant growth and survival as well as community assembly in response to water stress (reviewed by Reich 2014). When scaled up from measurements of individual plants and species, such traits may provide useful information regarding responses of communities and

ecosystems to climate change (Suding et al. 2008). Unfortunately, hydraulic traits are infrequently measured in community-scale trait surveys (Griffin-Nolan et al. 2018), likely due to the time-intensive measurement protocols they require (Sack et al. 2002; Brodribb and Holbrook 2003); thus, a key research need is the identification and validation of rapid, high-throughput methods for assessing drought tolerance that can be applied within and across plant functional types.

Leaf turgor loss point (π_{TLP}), the leaf water potential at which average cell turgor is lost and leaf wilting occurs, provides a wealth of physiological information pertaining to cell wall integrity, stomatal closure and, more generally, the extent to which plants can maintain metabolism as soil dries (Kramer and Boyer 1995; Bartlett et al. 2016; Meinzer et al. 2016). Given this and the strong correlation between π_{TLP} and water availability both within and between biomes, π_{TLP} is an ideal trait for assessing drought tolerance across broad spatial scales (Bartlett et al. 2012a). The traditional protocol for quantifying π_{TLP}, pressure–volume (p–v) curves, requires a lengthy procedure (up to 2 days to produce curves for 4–6 leaves) which greatly limits the number of species or locations that can be viably surveyed. Fortunately, π_{TLP} can be estimated from leaf osmotic potential at full turgor, the component of water potential related to cellular solute concentration and a strong determinant of π_{TLP} (Bartlett et al. 2012a). Leaf osmotic potential at full turgor (π_o) is typically quantified from p–v curves as well; however, Bartlett et al. (2012b) recently described a method for rapidly measuring π_o using a vapour pressure osmometer. The method has resulted in a 30- to 50-fold increase in the measurement speed of π_{TLP} and has since been used to quantify community-scale drought tolerance in tropical rainforests (Maréchaux et al. 2015). Since its publication, the osmometer method, and the linear model for predicting π_{TLP} from π_o, have exclusively been used in ecosystems dominated by woody species (Maréchaux et al. 2015; Esperón-Rodríguez et al. 2018) or crops (Mart et al. 2016) and has yet to be validated in herbaceous plant communities, such as grasslands. Indeed, several studies have cautioned that osmometer estimates of π_o may prove inaccurate for leaves with dense large vein networks or thin leaves with large midrib veins (i.e. grass leaf blades) as the inclusion of such veins in tissue sampling may lead to apoplastic dilution (Kikuta and Richter 1992; Maréchaux et al. 2016); thus, testing of the osmometer method within grasslands including such species is needed.

The grassland biome covers more than 30% of Earth's terrestrial surface and provides valuable ecosystem services such as carbon storage, soil stabilization, forage production, and wildlife habitat (Noy-Meir 1973; Field et al. 1998). Given that most grasslands are water-limited, they are an ideal study system for surveying drought tolerance and responses to future changes in Earth's hydrologic cycle (IPCC 2013). Here, we focus on grasslands of the American Great Plains, a region characterized by highly variable precipitation and a high frequency of climate extremes such as drought and flooding (Kunkel et al. 2013). Water availability will likely become more variable in this region as some of these grasslands are expected to experience more frequent "dust-bowl"-like conditions by the end of the century (Karl et al. 2009).

We conducted a survey of drought tolerance traits of common herbaceous plant species across three North American grasslands to address two main goals. First, we test the validity of the osmometer method (Bartlett et al. 2012b) for use on herbaceous plant species. Validation of this method will encourage community-scale surveys of drought tolerance across plant functional types, especially within a relatively drought-sensitive region (i.e. grasslands; Huxman et al. 2004; Knapp et al. 2015), as well as address recent concerns of scientific reproducibility (Baker 2016). Second, we assess the mechanistic value of π_o as a drought tolerance trait in grasslands. A central goal of trait-based ecology is to make generalized predictions of large-scale phenomenon (e.g. community assembly, nutrient cycling, dynamics of net primary production) using the composite traits of interacting organisms within a community (Shipley et al. 2016). Established links between species distributions, performance, and physiological traits are thus required, yet often difficult to identify (Paine et al. 2018). To this end, we test the hypothesis that π_o will be correlated with other mechanistic traits commonly used to describe leaf-level drought tolerance, namely leaf dry matter content (LDMC) and leaf vulnerability to hydraulic failure (Brodribb 2017). Additionally, we define the climatic extremes of species distributions and test the hypothesis that π_o is positively correlated with water availability (i.e. species with more negative π_o will predominately inhabit arid regions) (Bartlett et al. 2012a). The degree to which this correlation is driven by the driest or wettest extreme of a species distribution will highlight the relative influence of abiotic stress tolerance (i.e. water-limitation) or biotic stress tolerance (i.e. competition with more resource-acquisitive species), respectively, in controlling π_o of herbaceous species.

Materials and methods

Plant material

We collected nine species of graminoids and ten species of forbs/subshrubs (non-woody) from three native grassland sites (predominately mixed-grass prairie) across Wyoming and Kansas during mid-summer 2015 (Table 1). Six plant samples, including soil and a portion of the root system, were unearthed at each site, placed in a reservoir of water, and covered with large plastic bags ($n = 6$ pots/species/site).

Table 1 Herbaceous species surveyed in this study are shown along with collection sites, functional type, and trait means (SE). Traits include osmotic potential estimated from both an osmometer (π_{o*osm}) and p–v curves (π_{o*pv}), turgor loss point (π_{TLP}), vulnerability to cavitation (P_{50}), leaf dry matter content (LDMC), and apoplastic fraction (a_f)

Species	Code	Collection site[a]	Functional type	π_{o*osm} (MPa)	π_{o*pv} (MPa)	π_{TLP} (MPa)	P_{50} (MPa)	LDMC	A_f
Andropogon gerardii	ANGE	KNZ	Graminoid (C4 grass)	−1.2 (0.01)	−1.2 (0.04)	−1.7 (0.06)	−1.1	0.32	0
Bouteloua curtipendula	BOCU	HYS	Graminoid (C4 grass)	−1.8 (0.07)	−1.8 (0.11)	−2.5 (0.08)	−1.6	0.45	0.37
Bouteloua gracilis	BOGR	HPG	Graminoid (C4 grass)	−1.8 (0.02)	−1.7 (0.09)	−2.3 (0.12)	−1.1	0.46	0.16
Sorghastrum nutans	SONU	KNZ	Graminoid (C4 grass)	−0.9 (0.08)	−1.2 (0.06)	−1.6 (0.03)	−0.8	0.32	0.10
Sporobolus asper	SPAS	HYS	Graminoid (C4 grass)	−1.8 (0.12)	−1.6 (0.06)	−2.3 (0.12)	−2	0.41	0.11
Carex duriuscula	CADU	HPG	Graminoid (C3 sedge)	−2.7 (0.10)	−2.7 (0.16)	−3.2 (0.19)	−1.9	0.41	0.17
Hesperostipa comata	HECO	HPG	Graminoid (C3 grass)	−2.2 (0.06)	−2.2 (0.08)	−2.7 (0.13)	−2.3	0.44	0.39
Pascopyrum smithii	PASM	HPG	Graminoid (C3 grass)	−1.7 (0.02)	−1.6 (0.04)	−2.0 (0.07)	−1.8	0.38	0.20
Poa secunda	POSE	HPG	Graminoid (C3 grass)	−1.7 (0.11)	−1.5 (0.04)	−2.1 (0.12)	−	0.32	0.33
Leucocrinum montanum	LEMO	HPG	Monocot (forb)	−1.3 (0.06)	−0.8 (0.06)	−1.2 (0.11)	−	0.18	0.65
Astragalus drummondii	ASDR	HPG	Dicot (forb)	−0.7 (0.08)	−1.1 (0.12)	−1.5 (0.12)	−	0.24	0.58
Astragalus laxmannii	ASLA	HPG	Dicot (forb)	−1.0 (0.13)	−1.7 (0.09)	−2.2 (0.10)	−	0.26	0.26
Astragalus shortianus	ASSH	HPG	Dicot (forb)	−0.7 (0.07)	−0.7 (0.11)	−1.0 (0.15)	−	0.17	0.76
Linaria dalmatica	LIDA	HPG	Dicot (forb)	−0.6 (0.16)	−1.0 (0.09)	−1.3 (0.10)	−0.9	0.19	0.36
Mertensia lanceolata	MELA	HPG	Dicot (forb)	−0.9 (0.06)	−1.2 (0.08)	−1.5 (0.09)	−0.5	0.21	0.19
Penstemon albidus	PEAL	HPG	Dicot (forb)	−0.6 (0.01)	−1.3 (0.14)	−1.6 (0.13)	−1.3	0.27	0.18
Sphaeralcea coccinea	SPCO	HPG	Dicot (forb)	−1.0 (0.04)	−1.4 (0.13)	−1.9 (0.15)	−1.8	0.3	0.41
Artemisia frigida	ARFR	HPG	Dicot (subshrub)	−1.4 (0.04)	−1.1 (0.04)	−1.5 (0.04)	−	0.35	0.50
Eriogonum effusum	EREF	HPG	Dicot (subshrub)	−0.6 (0.08)	−1.1 (0.07)	−1.5 (0.11)	−	0.32	0.48

[a]Collection sites include a northern mixed-grass prairie (High Plains Grassland Research Center, HPG; mean annual precipitation [MAP] = 415 mm, mean annual temperature [MAT] = 7 °C, coordinates = 41°11′52″N, 104° 53′13″W) in Wyoming, a southern mixed-grass prairie (Hays Agricultural Research Center, HYS; MAP = 581 mm, MAT = 12.3 °C, coordinates = 39°5′9″N, 99°9′23″W) and a tallgrass prairie (Konza Prairie Biological Station, KNZ; MAP = 864 mm, MAT = 13 °C, coordinates 39°05′N, 96°35′W) in Kansas

Plants were left in the dark for ~ 12 h to allow leaves to fully rehydrate prior to p–v curve determination and osmometer measurements.

Osmometer method validation

Pressure–volume curves were measured on one leaf per plant sample (n = 6 leaves/species) using the bench drying method (Schulte and Hinckley 1985). A recently expanded mature leaf was wrapped in parafilm wax and cut near the leaf base (parafilm was weighed and subtracted from subsequent leaf weight measurements). Immediately after cutting, the leaf was placed in a Scholander-style pressure chamber (PMS Instruments, Albany, OR, USA) to measure leaf xylem water potential (Ψ_{leaf}). Following water potential determination, the leaf and parafilm were weighed on a micro-balance (± 0.1 mg, Ohaus Pioneer; Ohaus Corporation, Parsippany, NJ, USA). The leaf was then sealed in a plastic bag and placed in a dark drawer to allow slow dehydration. This process was repeated approximately 10 times for each leaf or until Ψ_{leaf} reached − 4 MPa. The leaf was then rehydrated, scanned for leaf area at 300 dpi (Epson Perfection V600, Epson America Inc., Long Beach, Ca, USA), dried for 48 h at 60 °C and weighed. Leaf area was calculated using ImageJ software (https://imagej.nih.gov/ij/). Turgor loss point (π_{TLP}), osmotic potential at full turgor (π_{o*pv}) and leaf capacitance (C_{leaf}) were calculated for 5–6 leaves following standard methods (Turner 1988; Koide et al. 1989) and averaged for each species. Fresh weight of hydrated and oven-dried leaves was used to calculate LDMC (g dry mass g^{-1} fresh mass).

Within 24 h of p–v curve determination, osmotic potential at full turgor was also estimated using a vapour pressure osmometer (π_{o*osm}) (VAPRO 5520 vapour pressure osmometer, Wescor, Logan, UT), following Bartlett et al. (2012b). Six leaves per species were clipped underwater and fully hydrated overnight prior to measuring π_{o*osm}. A leaf disc was sampled from each hydrated leaf using a 5-mm biopsy punch (Miltex DP-5 mm, Electrum Supply, Elkhart, IN), wrapped in tin foil, and submerged in liquid nitrogen for ~ 60 s to lyse the plant cell walls. The leaf disc was generally taken toward the apical portion of the leaf to avoid or minimize the sampling of large midrib veins, depending on leaf width. Bartlett et al. (2012b) warn of potential inaccuracies likely to arise when using the osmometer method on species with large midrib veins (e.g. grasses such as *Sorghastrum nutans*)

as the symplastic solution may become diluted by xylem water. When possible, the leaf disc was taken from a portion of the lamina without any midrib present (e.g. species with broad leaves). For species with leaves that were narrower than our biopsy punch, several leaves were aligned next to each other and the sample was taken across multiple leaves to ensure comparable disc sizes were sampled across species. Each disc was then punctured ~ 15 times using forceps to facilitate rapid equilibration in the osmometer chamber. Leaf discs were quickly placed in the osmometer chamber following puncturing to minimize evaporation (< 30 s between removal from liquid nitrogen and placement in osmometer chamber). Samples were left in the closed chamber for ~ 10 min to allow equilibration. Measurements were then made every two minutes until osmolarity reached equilibrium (<5 mmol kg^{-1} change in osmolarity between measurements). Osmolarity was then converted to osmotic potential at full turgor (π_{o*osm}) using the following equation: π_{o*osm} = osmolarity $* - 2.3958/1000$.

Bartlett et al. (2012b) outline possible discrepancies in osmometer measurements that can arise due to the opposing effects of apoplastic dilution (which leads to overestimations of π_{o*osm}) and cell wall dissolution (which leads to underestimations of π_{o*osm}). To account for such discrepancies, we calculated 'predicted π_{o*osm}' following a model presented by Bartlett et al. (2012b) which includes estimates of these effects:

$$\pi_{o*predicted} = (a \times \pi_{o*pv*af}) + (b \times LDMC) \\ + (c \times \pi_{o*pv*af} \times LDMC) + d \quad (1)$$

where, LDMC is a proxy for cell wall investment and thus dissolution, while $\pi_{o*pv*af}$ is an estimate of osmotic potential at full turgor (from p–v curves) corrected for apoplastic dilution, using apoplastic fraction (a_f) is a proxy ($\pi_{o*pv*af} = \pi_{o*pv} * (1 - a_f)$). p–v curve estimates of a_f were set to zero for one species (ANGE) as estimates were not significantly different from zero. A slope of 1 for the relationship between measured and predicted π_{o*osm} would indicate that accounting for apoplastic dilution and cell wall dissolution corrects this bias in osmometer measurements (Bartlett et al. 2012b).

Leaf hydraulic conductance

Leaf hydraulic vulnerability curves were produced for 12 of the 19 focal species, including both graminoids and forbs/subshrubs, following the rehydration kinetics method (Brodribb and Holbrook 2003). The methodology described here is for graminoids, as vulnerability curves for forbs, subshrubs, and one sedge (*Carex duriuscula*) were taken from previously collected data (Ocheltree in review). Several tillers, each with at least two recently emerged leaves of comparable size, were clipped from the rehydrated samples and

placed on a bench to dry slowly. Drying time varied from 30 s to 3 h depending on the species and the desired level of dehydration. Prior to hydraulic conductance measurements, the tiller was sealed in a plastic bag and placed in a dark drawer for 2–3 min to allow any water potential gradients across a single leaf to equilibrate. The more apical leaf was removed from the stem with a razor and placed in a pressure chamber to determine initial leaf water potential (Ψ_0). The second leaf was removed by cutting under filtered de-ionized water that had been de-gassed for 1 h and then rehydrated for a pre-determined amount of time (5–120 s depending on Ψ_0). The leaf was then re-cut slightly above the water line and placed in a pressure chamber to determine final rehydrated leaf water potential (Ψ_f). Leaf hydraulic conductance (K_{leaf}) was then calculated using initial and final leaf water potential as well as average capacitance (C_{leaf}; $n = 6$) quantified from p–v curves:

$$K_{leaf} = \frac{C_{leaf} * \ln\left[\frac{\varphi_0}{\varphi_f}\right]}{t} \quad (2)$$

where t is the rehydration time in seconds. K_{leaf} was calculated for 30–40 leaves varying in hydration status and regressed against Ψ_0. Maximum conductance (K_{max}) was estimated as the mean of the five highest values of K_{leaf} between Ψ_0 of -0.5 and -1 MPa. Leaf hydraulic vulnerability curves were produced by fitting logarithmic, linear, exponential, and sigmoidal models to data binned and averaged to 0.5 MPa intervals and selecting the model with the lowest Akaike Information Criteria (AIC; see Table S1 for AIC values). This model was used to calculate the leaf water potential at which K_{leaf} decreases to 50% of K_{max} (P50, in MPa). Vulnerability curves were made for a subset of graminoids in this study (Fig. S1), while P_{50} values for forbs/shrubs were taken from Ocheltree (in review).

Bioclimatic envelopes

Bioclimatic envelopes of temperature and precipitation were generated using the geographic range of each species. Spatial information on all reported occurrences of each species was downloaded from the Global Biodiversity Information Facility (GBIF; www.gbif.org). The number of reported occurrences ranged from 90 to 8259 with an average of 1193 occurrences/species. Climatic data from the nearest 0.5-km grid cell of each reported occurrence were collected from the WorldClim database (http://www.worldclim.org/biocl im). Because GBIF data are spatially biased and one region can be over-represented in a data set (Beck et al. 2014), we subsampled the climate data to remove this bias. If multiple occurrences fell within the same grid cell of climate data from WorldClim, that grid cell was only used once in our

analysis. Further, the occurrence data were filtered to remove any incorrect entries that reported occurrences in aquatic environments (i.e. large bodies of water). We focused on variables including estimates of temperature and precipitation seasonality as well as annual summaries of temperature and precipitation (see Table S2 and the WorldClim database for a full list of climatic variables). The 5th and 95th quantiles of each variable were calculated from data compiled for all recorded occurrences to quantify bioclimatic envelopes that define the climatic extremes of a species' inhabited range. For example, the 5th quantile of 'precipitation during the wettest month' represents the precipitation during the wettest month in the driest locations of a species range. These bioclimatic envelope parameters have been shown to be more biologically relevant than regional annual climate statistics (Ocheltree et al. 2016).

Data analyses

Univariate linear regression analyses were used to test for relationships among π_{TLP}, π_{o*pv}, and π_{o*osm}. The assumptions of linear regression (skewness, heteroscedasticity, etc.) were met for all models presented in this study. The slope and intercept of the models presented by Bartlett et al. (2012b) were compared to 95% confidence intervals (CI) of the slope and intercept of the models presented here. The PRESS and RMSE statistics for all method comparison models are available in Table S3. The most parsimonious model for estimating both π_{o*pv} and π_{TLP} was determined by calculating AICc values for linear mixed effects models including LDMC, a_p, π_{o*osm} and all possible interactions as fixed effects (AICc values in Table S4). Leaf osmotic potential at full turgor (π_{o*osm}) was also regressed against P_{50} and LDMC to investigate correlations among these functional traits. Traits of different plant functional types (graminoids vs. forb/subshrub) were compared using t tests. Additionally, hydraulic trait mean values from Bartlett et al. (2012b) were compared to the range of hydraulic trait values assessed in this study. Relationships between species-specific bioclimatic envelopes and π_{o*osm} were also assessed using a Pearson's correlation matrix ('cor' function in base R). R statistical software version 3.4.4 was used for all statistical analyses.

Results

Osmometer method validation

Leaf turgor loss point and osmotic potential at full turgor calculated from p–v curves were highly correlated among common herbaceous species within central US grasslands, with 96% of the variation in π_{TLP} explained by π_{o*pv} (Fig. 1). Additionally, π_{o*pv} was highly correlated with osmotic

potential estimated from a vapour pressure osmometer (π_{o*osm}) (Fig. 2), with the slope and intercept not significantly different from that presented by Bartlett et al. (2012b); however, this model did diverge from a 1:1 relationship indicating some bias in osmometer measurements. Using Eq. 1, we tested whether the divergence from a 1:1 line in this method comparison could be explained by the opposing effects of apoplastic dilution and cell wall dissolution. The relationship between $\pi_{o*predicted}$ and π_{o*osm} ($r^2 = 0.78$) did not differ significantly from a 1:1 relationship, indicating no bias after correcting for these factors (Fig. 3). Nonetheless, model selection for predicting π_{o*pv} from all combinations of fixed effects (π_{o*osm}, a_f, and LDMC, plus interactions) selected a model with just π_{o*osm} as the most parsimonious (AICc = 10.57; Table S4) with the amount of variance explained only increasing by 13% with the inclusion of a_f and LDMC (plus interactions).

Leaf osmotic potential at full turgor measured with an osmometer was highly correlated with leaf turgor loss point across several common grassland species including graminoids, forbs and subshrubs (Fig. 4a). This linear model for predicting π_{TLP} of predominantly herbaceous species is nearly identical to the woody species model presented by Bartlett et al. (2012b), with a minor offset for the y intercept (− 0.21 MPa). Additionally, the slope and intercept of their model fall within the 95% CI of the grassland model presented here. The strength of the grassland model was
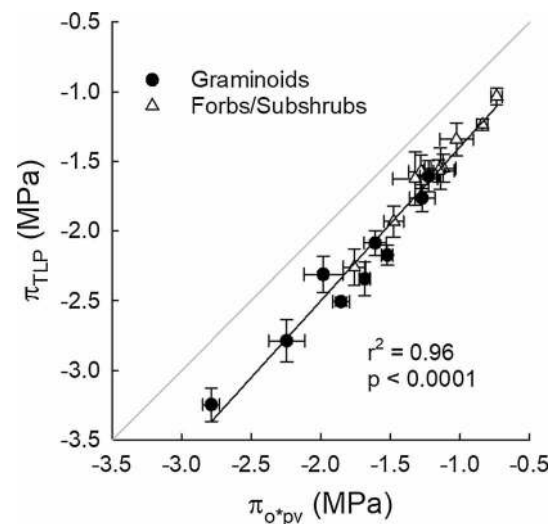
Fig. 1 Leaf turgor loss point is largely controlled by leaf osmotic potential at full turgor, the component of leaf water potential determined by cellular solute concentrations. A strong linear relationship between osmotic potential at full turgor (π_{o*pv}) and osmotic potential at turgor loss point (π_{TLP}) estimated from pressure–volume curves is shown for largely herbaceous grassland species including graminoids, forbs, and subshrubs. The black line represents this model: $\pi_{TLP} = 1.103\pi_{o*pv} - 0.294$, while the grey line represents the 1:1 line and bi-directional error bars represent standard error
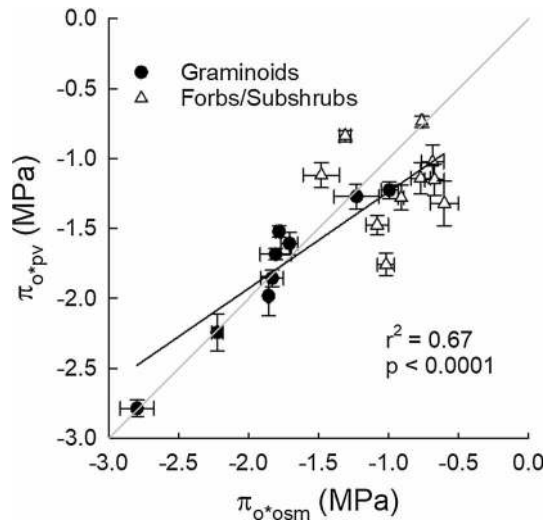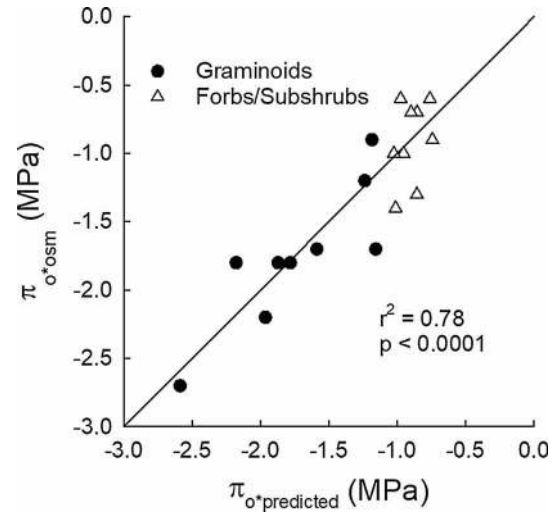
Fig. 2 Osmotic potential at full turgor measured with a vapour pressure osmometer (π_{o^*osm}) predicts that estimated from p–v curves (π_{o^*pv}) with a slight deviation from the 1:1 line. The model shown here ($\pi_{o^*pv} = 0.690\pi_{o^*osm} - 0.5481$; black line) does not differ significantly from a similar model presented for woody species ($\pi_{o^*pv} = 0.690\pi_{o^*osm} - 0.5481$; Bartlett et al. 2012b) based on the 95% CI of the slope (0.45, 0.92) and intercept (-0.8954093, -0.2007442). Graminoid species fall along the 1:1 line (grey line), while much of the scatter is due to variability in forbs/subshrubs. Bidirectional error bars represent standard error
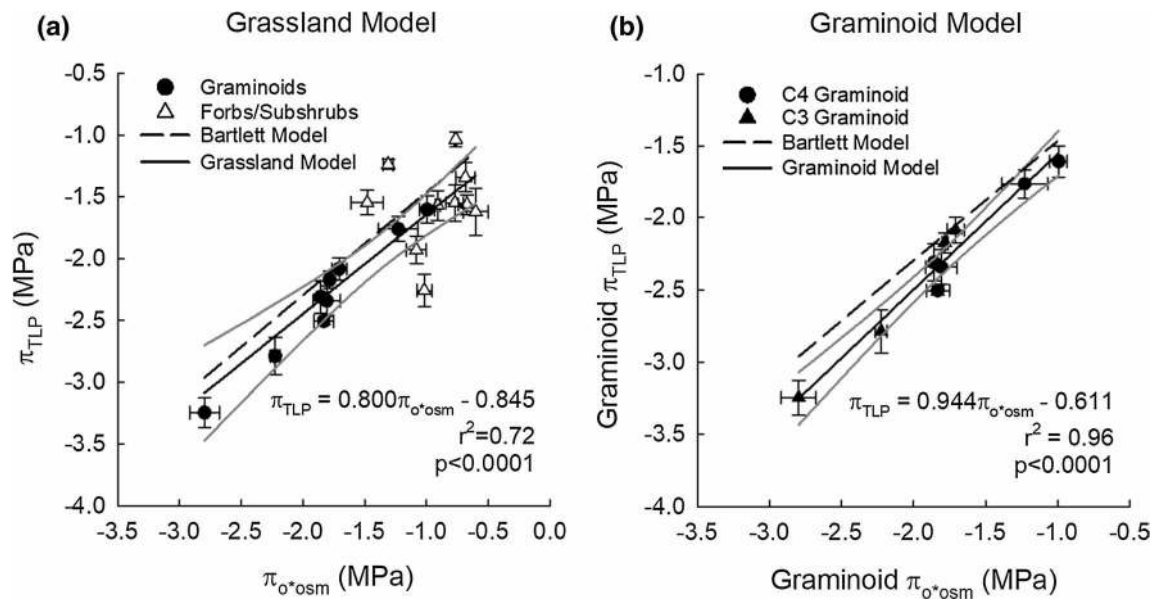

Fig. 3 Correcting for discrepancies that arise from osmometry (see the departure from the 1:1 line in Fig. 2), π_{o^*osm} was recalculated using Eq. 2 (taken from Bartlett et al. 2012b). Osmometry can lead to over- and underestimations of π_o due to apoplastic dilution and cell wall dissolution, respectively. Here, predicted osmotic potential at full turgor ($\pi_{o^*predicted}$) was calculated from a model that includes estimates of cell wall dissolution (leaf dry matter content as a proxy, LDMC), apoplastic fraction, and their interaction. The fitted regression between measured π_{o^*osm} and $\pi_{o^*predicted}$ has a slope of 1.0 ± 0.12 SE ($\pi_{o^*osm} = 1.0 \pi_{o^*predicted} - 5.6e^{-6}$; plotted black line), as does the relationship including solely graminoids (slope $= 0.9 \pm 0.23$ SE; see Table S2), indicating no bias after correcting for these factors. The counterbalancing effects of apoplastic dilution and cell wall dissolution suggest the osmometer method is robust for graminoid leaves (graminoids fall along the 1:1 line in Fig. 2); however, the net effect of LDMC and a_f should be considered for other types of leaves.
$\pi_{o^*predicted} = -1.2684 * \pi_{o^*pv*af} + 1.4875 * LDMC + 5.2601 * \pi_{o^*pv*af} * LDMC - 1.2147$

improved when forbs and subshrubs were excluded, with 96% of the variation in graminoid π_{TLP} explained by π_{o^*osm} (Fig. 4b)—this relationship also did not differ from that of Bartlett et al. (2012b). Among forbs/subshrubs, we did not observe a significant relationship between π_{TLP} and π_{o^*osm}.

Mechanistic value of π_o

We found significant differences in trait values between plant functional types (PFT; graminoids vs. forbs/subshrubs). Graminoids had significantly lower pressure potential for all parameters (π_{TLP}, π_{o^*pv} and π_{o^*osm}) than forbs/subshrubs (Fig. 5), with this PFT difference similar in magnitude to the regional differences observed by Bartlett et al. (2012b) between species sampled from a tropical forest site (annual rainfall = 1532 mm) and a common garden near UCLA (annual rainfall = 450 mm). These average differences between PFTs contributed substantially to the correlations between pressure potential parameters (e.g., π_{TLP} and π_o) among species (Figs. 1, 2, 3). Graminoid species also had significantly higher LDMC compared to forbs/subshrubs (mean = 0.39 and 0.25 g g^{-1}, respectively; t test, $p < 0.001$). No statistical comparisons of P_{50} across PFTs were tested due to the small sample size for forbs/subshrubs ($n = 3$; Table 1).

Osmometer estimates of leaf osmotic potential at full turgor were highly correlated with other hydraulic and morphological traits that are indicative of drought tolerance. Specifically, π_{o^*osm} was positively correlated with vulnerability to hydraulic failure (P_{50}; see Fig. S1 for vulnerability curves), and negatively correlated with leaf dry matter content (LDMC), suggesting there may be coordination among leaf drought tolerance characteristics of these species (Fig. 6). Additionally, LDMC was negatively correlated with P_{50} ($r^2 = 0.37$; $p = 0.02$).

The bioclimatic envelopes assessed in this study represent climatic boundaries of a species distribution with high and low quantiles indicating the climate extremes that species experiences across their observed range. For graminoids, the bioclimatic envelope that explained the most variability in π_{o^*osm} was mean annual precipitation (MAP) at the wettest extremes (95th quantile) of a species distribution (Fig. 7; MAP$_{95th}$ was also significantly correlated with π_{o^*pv}; $r^2 = 0.60$). This significant positive relationship indicates that π_{o^*osm} was less negative for graminoid species that occupy

(a) Grassland Model

$\pi_{TLP} = 0.800\pi_{o*osm} - 0.845$
$r^2 = 0.72$
$p < 0.0001$

(b) Graminoid Model

$\pi_{TLP} = 0.944\pi_{o*osm} - 0.611$
$r^2 = 0.96$
$p < 0.0001$

Fig. 4 A linear model for predicting leaf turgor loss point (π_{TLP}) among grassland species using osmotic potential at full turgor estimated from a vapour pressure osmometer (π_{o*osm}). **a** The slope and intercept of the linear model developed by Bartlett et al. ($\pi_{tlp} = 0.832\pi_{osm} - 0.631$; dashed line) falls within the 95% CI of the slope (0.5552126, 1.0460131) and intercept (− 1.2050772, − 0.4852862) of the grassland model shown here (black line; grey line represents the 95% CI). **The** linear model equation depicted on the figure is for the grassland model, which includes graminoids, forbs

and subshrubs. **b** The linear model including only graminoid species also does not differ significantly from the Bartlett model (dashed line) which falls within the 95% CI of the slope (0.7793554, 1.1086195) and intercept (− 0.9190000, − 0.3034649) of the graminoid model shown here (black line; grey line represents the 95% CI). No significant relationship was found for forbs/subshrubs alone. Symbols represent photosynthetic pathway (C4 vs. C3). Bi-directional error bars represent standard error
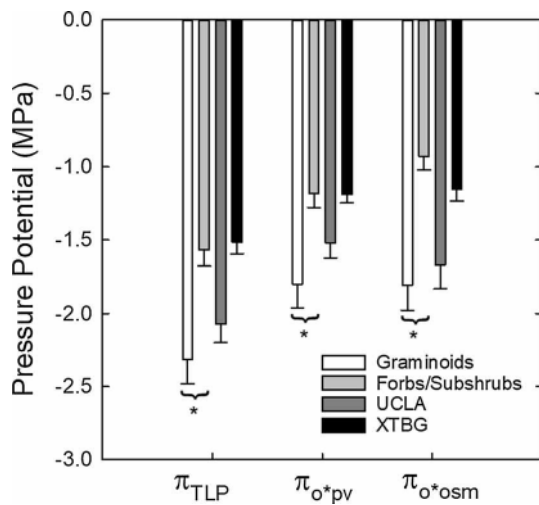

Fig. 5 Turgor loss point (π_{TLP}) and osmotic potential at full turgor measured from pressure–volume curves (π_{o*pv}) and a vapour pressure osmometer (π_{o*osm}) are shown grouped by plant functional type (graminoids and forbs/subshrubs; mean ± SE). Forbs/subshrub species have significantly higher pressure potentials for each trait compared to graminoid species ($p < 0.05$; denoted by *). Also shown are the pooled mean (± SE) for the species used in the Bartlett et al. (2012b) model sampled from two separate locations: a common garden near University of California Los Angeles (UCLA; annual rainfall = 450 mm) and a tropical forest plant community at Xishuangbanna Botanic Garden in China (XTBG; annual rainfall = 1532 mm)

sites characterized by high annual rainfall. This relationship was driven by the wet extremes of a species distribution as there was only a moderately significant relationship between graminoid π_{o*osm} and the 5th quantile of MAP ($p = 0.08$). Temperature was not a significant predictor of graminoid π_{o*osm}. When PFTs were combined, however, the only significant predictor of π_{o*osm} was temperature; a weak positive relationship ($r^2 = 0.18$; $p = 0.04$) was observed between π_{o*osm} and the 5th quantile of temperature during the wettest quarter of the year. Given that most precipitation in grasslands falls within the spring/summer growing season (Rosenberg 1987), this bioclimatic envelope parameter represents the coldest growing season temperature extremes a species can tolerate. A positive relationship indicates that π_{o*osm} is more negative for species capable of growing in areas with low growing season temperatures. No significant trait×climate relationships were observed for forbs/subshrubs separately.
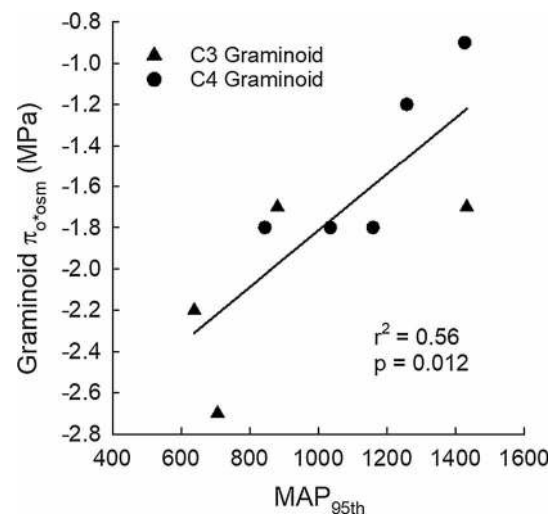
Discussion

Osmometer method validation

Leaf hydraulic traits, such as π_o and π_{TLP}, of trees are well correlated with spatial variability in annual moisture
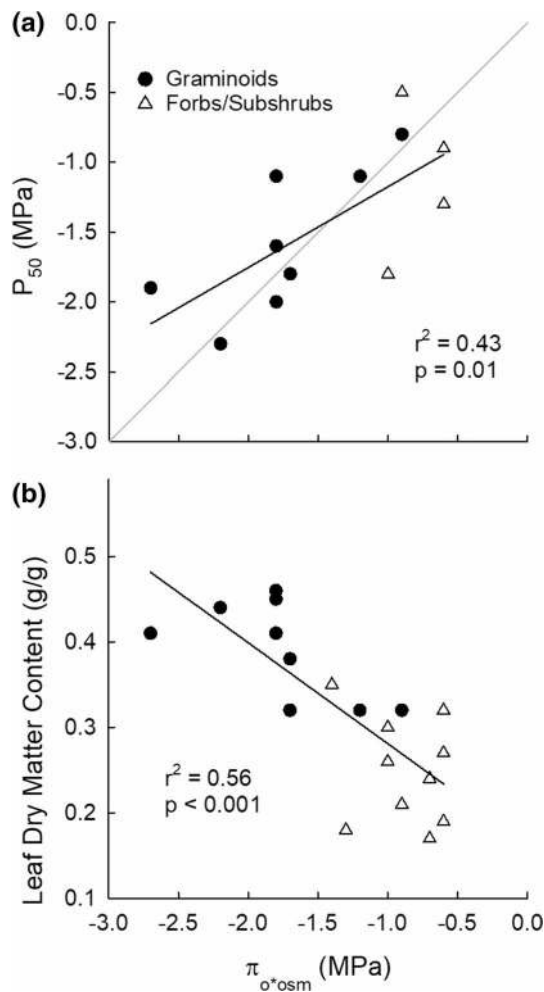
Fig. 6 Osmotic potential at full turgor can be rapidly estimated from a vapour pressure osmometer (π_{o*osm}) and is correlated with other mechanistic plant traits such as, **a** the leaf water potential at 50% loss of hydraulic conductance (P_{50}) and **b** leaf dry matter content (LDMC). The 1:1 line is shown as a grey line

Fig. 7 Mean annual precipitation at the wettest extremes of a species distribution (MAP_{95th}) explained a significant portion of interspecific variability (56%) in osmotic potential at full turgor measured with an osmometer (π_{o*osm}). A positive relationship indicates that species with lower π_{o*osm} (more negative) are found in drier regions of the central US. The wet extreme (i.e. 95th quantile) suggests that resource allocation to drought tolerance (i.e. low π_{o*osm}) is beneficial along an aridity gradient only until water becomes less limiting, at which point more mesic species with higher growth rates outcompete xeric species. At the dry extreme of species bioclimatic envelopes (5th quantile), π_{o*osm} was only moderately significantly correlated with precipitation during the wettest quarter of the year ($p = 0.08$)

availability as well as species distributions across moist and dry biomes (Bartlett et al. 2012a). The osmometer method for rapidly estimating these traits in woody species has facilitated community-scale surveys of leaf-level drought tolerance in several forest ecosystems (Bartlett et al. 2012b; Maréchaux et al. 2015); however, concerns about the utility of this method for estimating osmotic potential at full turgor of thin leaves with large midribs (e.g. graminoids) have prevented its application to a wide range of plant functional groups. Several of the graminoid species surveyed in this study have large leaf midribs, a characteristic that has the potential to diminish the proportion of extra-xylary water in the sample placed in the osmometer chamber. Considering that xylem typically contains lower sugar concentrations than other cells in the leaf (Peuke et al. 2001), the inclusion of the midrib in a sample could lead to an overestimation of

π_o when using an osmometer compared to estimates from p–v curves (Bartlett et al. 2012b); however, we found no evidence of this potential bias among the species we sampled. We observed a significant relationship between osmotic potential at full turgor measured with an osmometer (π_{o*osm}) and p–v curves (π_{o*pv}) with all graminoid species falling along the 1:1 line (Fig. 2). A large midrib does not necessarily mean there is a larger proportion of xylem conduits relative to solute-rich mesophyll cells. For instance, large midribs typically have multiple vascular bundles that are similar in size and density to bundles outside of the midrib (Fig S2; also see Evert and Eichhorn 2013). The midrib also has a large amount of parenchyma tissue which contributes to total leaf osmotic potential at full turgor. Thus, the inclusion of the midrib may not necessarily lower the proportion of extra-xylary water in a sample.

The slope and intercept of the relationship shown in Fig. 2 is not significantly different from the relationship presented by Bartlett et al. ((2012b)—Fig. 2, within). This relationship differs significantly from a 1:1 relationship indicating clear bias in osmometry. Such bias is expected in osmometer measurements of π_o due to the net effect apoplastic dilution and cell wall dissolution (Bartlett et al. 2012b). Rupturing of plant cell walls during sample processing causes water from the apoplast to dilute the sample leading to overestimations

of π_o. Additionally, underestimation of π_o can occur as disturbed cell wall materials dissolve into the sample solution. We accounted for these opposing effects following Eq. 1 and found a 1:1 relationship between measured and predicted π_{o*osm} (Fig. 3), which is in line with measurements on leaves from woody species (Bartlett et al. 2012b). This highlights the robustness of this method as well as the importance of considering species-specific leaf vein networks and the net effect of apoplastic dilution and cell wall dissolution, which might change the fitted regression across leaf types.

We provide evidence that the osmometer method developed by Bartlett et al. (2012b) can be used to estimate leaf turgor loss point in herbaceous species commonly found in central US grasslands:

$$\pi_{tlp} = 0.80\pi_{o*osm} - 0.845 \qquad (3)$$

Not only was the relationship between π_{TLP} and π_{o*osm} statistically significant (Fig. 4a), the model parameters were nearly identical to those presented by Bartlett et al. (2012b) for woody species, suggesting the same linear model can be applied across plant functional types. The striking similarity between the 'Grassland' and 'Bartlett' models is likely a result of: (1) the similar range in drought tolerance assessed in the two studies (Fig. 5); (2) the fact that this method samples similar proportions of mesophyll tissue despite anatomical differences between dicots and monocots; and (3) the dominant role of osmotic potential at full turgor in explaining turgor loss point across all plants at a global scale (Bartlett et al. 2012a), and perhaps more so across plant functional types within communities (Fig. 1). Our results show that 72% of the variation in π_{TLP} across all species and 96% of the variation in π_{TLP} of graminoids were explained using the osmometer method, providing strong support for the validity of this technique both across functional groups and within graminoids. The lack of a correlation between π_{TLP} and π_{o*osm} for forbs/subshrubs may be due to the smaller range in π_{TLP} and π_{o*osm} values sampled. Given that forb species were all measured within the same site (**HPG**), we recommend additional measurements of π_{TLP} and π_{o*osm} of forb species across broad spatial aridity gradients. We suggest caution in interpreting π_{o*osm} of forb species until additional results on this growth form have been reported. We recommend using the following linear model for estimating leaf turgor loss point from π_{o*osm} of common C3 and C4 grass species:

$$\pi_{tlp} = 0.944\pi_{o*osm} - 0.611 \qquad (4)$$

Mechanistic value of π_o

This rapid measure of leaf drought tolerance for herbaceous species is especially useful if these traits can help us understand the ecological strategies of plants, which are often identified through analyses of trait covariation (Wright et al.

2004). We observed a negative relationship between π_{o*osm} and LDMC, a commonly measured leaf trait indicative of resource conservation strategies and leaf construction costs (Poorter and Garnier 1999) (Fig. 6). Large values of LDMC can result from either a large structural investment in leaf tissue and/or high concentrations of non-structural carbohydrates. Structural investments are generally considered to result from extensive cell wall investment, such as thick-walled xylem or a large proportion of small diameter vessels. The negative relationship we observed likely reflects both components of LDMC. We would expect plants with more negative π_{o*osm} to have a higher concentration of non-structural carbohydrates or other osmolytes. In addition, especially in ecosystems with more severe or persistent water stress, plants that invest in more negative π_{o*osm} (i.e. lower turgor loss point) tend to further bolster their drought tolerance by investing in xylem that is resistant to hydraulic failure (Zhu et al. 2018), which is characterized by conduits with thick walls relative to their lumen diameter (Blackman et al. 2010). Indeed, we did find a negative relationship between LDMC and resistance to hydraulic failure (P_{50}), which may reflect this investment in xylem. We also observed a significant relationship between π_{o*osm} and P_{50}, a valuable trait for defining hydraulic safety vs. efficiency tradeoffs and re-growth capabilities of grasses following drought (Ocheltree et al. 2016). Leaf resistance to hydraulic failure (i.e. P_{50}) is largely determined by leaf vein architecture (Scoffoni et al. 2011); thus, the osmometer method can provide both a valuable proxy for π_{TLP} as well as information about aspects of drought tolerance more closely associated with leaf structural investments (LDMC and P_{50}).

Trait–environment relationships are key for understanding species responses to climate change (Suding et al. 2008). In forested biomes, lower values π_o are associated with high aridity (Bartlett et al. 2012a; Zhu et al. 2018). For herbaceous plants, identifying climate variables that explain the distributions of species traits can be more difficult given the ability of these plants to occupy microsites within a landscape (Ricklefs and Latham 1992). Despite these potential limitations, we did find significant trait–environment relationships for π_{o*osm} of graminoids and PFTs combined. Graminoid species that more exclusively occupy xeric regions (low MAP) tend to have lower π_{o*osm} (Fig. 7) suggesting that low π_{o*osm} helps plants to survive and reproduce where water is limiting, as observed for woody species (Bartlett et al. 2012a); however, MAP at the driest extremes of graminoid species distributions (MAP_{5th}) was not significantly correlated with π_{o*osm}, while MAP of the wettest extremes was (Fig. 7); this indicates that the distribution of drought tolerance traits for graminoids may be determined by competitive pressures that are maximized at the wetter end of their distribution where more acquisitive faster growing species dominate grassland communities. Allocating

resources to lower π_{o*osm} is indeed advantageous in drier climates; however, it may prevent graminoid species from inhabiting mesic areas where the costs of such strategies (slower growth rates) outweigh the benefits.

Across functional types, temperature was the only significant climatic predictor of π_{o*osm}. Specifically, temperature of the wet season for the coldest regions of a species distribution explains only 18% of the variability in π_{o*osm} across PFTs. This significant, albeit weak, relationship may simply reflect functional type differences (graminoids vs. forbs/subshrubs; Fig. 5) and the temperature constraints on the geographic distribution of C4 vs. C3 plants (Sage and Monson 1999; Edwards and Still 2008) or adaptations for freezing tolerance (Liu and Osborne 2008). The lack of any significant trait × climate relationship for forbs/subshrubs highlights the potential lack of utility of this trait for understanding drought responses of these functional types, which tend to rely more on deep roots rather than drought-tolerant leaves (Weaver 1958).

Until additional studies evaluate the relationship between π_{TLP} and π_{o*osm} within communities, including both herbaceous and woody-dominated ecosystems, it will remain unclear to what extent the tight coupling of π_{TLP} and π_{o*osm} across broad geographic scales and phylogenetic groups (sensu Bartlett et al. 2012b and this study) is representative of: (1) convergent, but partly independent responses of both π_{TLP} and π_{o*osm} to environmental gradients in space and time, or (2) stringent biophysical or ecological constraints on covariance between π_{TLP} and π_{o*osm} that operate independent of the spatial or phylogenetic scope of sampling. In other words, caution must be applied when interpreting the functional equivalence of π_{TLP} and π_{o*osm} among species within any given community. Additionally, although π_{TLP} and π_{o*osm} represent promising traits for capturing differences in the ability of plants to maintain function and keep tissues alive at low water potentials, they do not capture drought-avoidance strategies that enable plants to maintain high leaf water potential through water conservation or deep rooting profiles (Levitt 1980; Mitchell et al. 2016). Furthermore, π_{TLP} and π_{o*osm} are measured on fully rehydrated plants, which fails to capture the trait plasticity exhibited by some species when partially dehydrated. For example, π_{TLP} can change by > 1.0 MPa in *Juniperus monosperma* within several hours, primarily due to osmotic adjustment (Meinzer et al., 2014). On a global scale, however, osmotic adjustment typically accounts for up to a 0.5 MPa change in π_{TLP} (Bartlett et al., 2014), and has little influence on species' ranks with respect to leaf-level drought tolerance, but there are clearly exceptions that should be considered when interpreting π_{TLP} and π_{o*osm} as indices of plant responses to drought.

In summary, leaf-level drought tolerance of herbaceous species can be measured accurately and rapidly using the osmometer method. We provide evidence that π_{o*osm} predicts π_{TLP} of herbaceous species from a linear model nearly identical to that of woody species ($\pi_{tlp} = 0.80\pi_{o*osm} - 0.845$) and is well correlated with two other traits indicative of drought tolerance (LDMC and P_{50}) as well as species-specific distributions across gradients of precipitation. There is an urgent need for rapid techniques to assess plant community-scale drought tolerance (Griffin-Nolan et al. 2018) as a hotter and drier climate will become the norm for many of Earth's ecosystems (IPCC 2013). To make predictions of how different plant functional types will respond to increased drought frequency and intensity, we need to identify baseline metrics of drought tolerance that are comparable across the plant kingdom. The osmometer method makes community-scale surveys of drought tolerance possible, which will improve trait-based predictions of ecosystem responses to climate change and allow for a more integrative understanding of plant functional strategies for dealing with water stress.

Author contribution statement All authors contributed substantially to data collection and the conception of the experiment. RJGN and TWO conducted the analyses and wrote the initial draft of this manuscript; other authors provided editorial advice.

References

Baker M (2016) Is there a reproducibility crisis? A nature survey lifts the lid on how researchers view the 'crisis' rocking science and what they think will help. Nature 533(7604):452–455

Bartlett MK, Scoffoni C, Sack L (2012a) The determinants of leaf turgor loss point and prediction of drought tolerance of species and biomes: a global meta-analysis. Ecol Lett 15(5):393–405

Bartlett MK, Scoffoni C, Ardy R, Zhang Y, Sun S, Cao K, Sack L (2012b) Rapid determination of comparative drought tolerance traits: using an osmometer to predict turgor loss point. Methods Ecol Evol 3(5):880–888

Bartlett MK, Zhang Y, Kreidler N, Sun S, Ardy R, Cao K, Sack L (2014) Global analysis of plasticity in turgor loss point, a key drought tolerance trait. Ecol Lett 17:1580–1590

Bartlett MK, Zhang Y, Yang J et al (2016) Drought tolerance as a driver of tropical forest assembly: resolving spatial signatures for multiple processes. Ecology 97:503–514

Beck J, Böller M, Erhardt A, Schwanghart W (2014) Spatial bias in the GBIF database and its effect on modeling species' geographic distributions. Ecol Inf 19:10–15

Blackman CJ, Brodribb TJ, Jordan GJ (2010) Leaf hydraulic vulnerability is related to conduit dimensions and drought resistance across a diverse range of woody angiosperms. New Phytol 188:1113–1123

Brodribb TJ (2017) Progressing from 'functional' to mechanistic traits. New Phytol 215(1):9–11

Brodribb TJ, Holbrook NM (2003) Stomatal closure during leaf dehydration, correlation with other leaf physiological traits. Plant Physiol 132(4):2166–2173

Dai A (2011) Drought under global warming: a review. WIREs Clim Change 2:45–65

Dai A (2013) Increasing drought under global warming in observations and models. Nat Clim Change 3:52–58

Edwards EJ, Still CJ (2008) Climate, phylogeny and the ecological distribution of C4 grasses. Ecol Lett 11(3):266–276

Esperón-Rodríguez M, Curran TJ, Camac JS, Hofmann RW, Correa-Metrio A, Barradas VL (2018) Correlation of drought traits and the predictability of osmotic potential at full leaf turgor in vegetation from New Zealand. Austral Ecol 43:397–408

Evert RF, Eichhorn SE (2013) Raven biology of plants. Freeman and Co, Chicago, pp 598–599

Field CB, Behrenfeld MJ, Randerson JT, Falkowski P (1998) Primary production of the biosphere: integrating terrestrial and oceanic components. Science 281(5374):237–240

Griffin-Nolan RJ, Bushey JA, Carroll CJW et al (2018) Trait selection and community weighting are key to understanding ecosystem responses to changing precipitation regimes. Funct Ecol 00:1–11. https://doi.org/10.1111/1365-2435.13135

Huxman TE, Smith MD, Fay PA, Knapp AK, Shaw MR, Loik ME, Smith SD, Tissue DT, Zak JC, Weltzin JF, Pockman WT (2004) Convergence across biomes to a common rain-use efficiency. Nature 429(6992):651

IPCC (2013) Climate Change 2013. The physical science basis. Working group I contribution to the fifth assessment report of the intergovernmental panel on climate change. Stocker TF, Qin D, Plattner GK, Tignor MMB, Allen SK, Boschung J, Nauels A, Xia Y, Bex V Midgley PM, eds. Cambridge University Press, Cambridge

Karl TR, Melillo JM, Peterson TC (2009) Global climate change impacts in the United States: a state of knowledge report from the US Global Change Research Program. Cambridge University Press, Cambridge

Kikuta SB, Richter H (1992) Leaf discs or press saps? A comparison of techniques for the determination of osmotic potentials in freeze-thawed leaf material. J Exp Bot 43(8):1039–1044

Knapp AK, Carroll CJ, Denton EM, La Pierre KJ, Collins SL, Smith MD (2015) Differential sensitivity to regional-scale drought in six central US grasslands. Oecologia 177(4):949–957

Knapp AK, Ciais P, Smith MD (2017) Reconciling inconsistencies in precipitation–productivity relationships: implications for climate change. New Phytol 214(1):41–47

Koide RT, Robichaux RH, Morse SR, Smith CM (1989) Plant water status, hydraulic resistance and capacitance. Plant physiological ecology. Springer, New York, pp 161–183

Kramer PJ, Boyer JS (1995) Water relations of plants and soils. Academic Press, San Diego

Kunkel KE, Stevens LE, Stevens SE et al (2013) Regional Climate Trends and Scenarios for the U.S. National Climate Assessment. Part 4. Climate of the U.S. Great Plains. NOAA Technical Report NESDIS 142-4, 82

Levitt J (1980) Responses of plants to environmental stresses. Volume II. Water, radiation, salt, and other stresses. Academic Press, New York

Liu MZ, Osborne CP (2008) Leaf cold acclimation and freezing injury in C3 and C4 grasses of the Mongolian Plateau. J Exp Bot 59(15):4161–4170

Maréchaux I, Bartlett MK, Sack L, Baraloto C, Engel J, Joetzjer E, Chave J (2015) Drought tolerance as predicted by leaf water potential at turgor loss point varies strongly across species within an Amazonian forest. Funct Ecol 29(10):1268–1277

Maréchaux I, Bartlett MK, Gaucher P, Sack L, Chave J (2016) Causes of variation in leaf-level drought tolerance within an Amazonian forest. J Plant Hydraul 31(3):e004

Mart KB, Veneklaas EJ, Bramley H (2016) Osmotic potential at full turgor: an easily measurable trait to help breeders select for drought tolerance in wheat. Plant Breed 135(3):279–285

Meinzer FC, Woodruff DR, Marias DE, McCulloh KA, Sevanto S (2014) Dynamics of leaf water relations components in co-occurring iso-and anisohydric conifer species. Plant, Cell Environ 37(11):2577–2586

Meinzer FC, Woodruff DR, Marias DE, Smith DD, McCulloh KA, Howard AR, Magedman AL (2016) Mapping 'hydroscapes' along the iso-to anisohydric continuum of stomatal regulation of plant water status. Ecol Lett 19(11):1343–1352

Mitchell PJ, O'grady AP, Pinkard EA et al (2016) An ecoclimatic framework for evaluating the resilience of vegetation to water deficit. Glob Change Biol 22(5):1677–1689

Noy-Meir I (1973) Desert ecosystems: environment and producers. Annu Rev Ecol Syst 4(1):25–51

Ocheltree TW, Nippert JB, Prasad PV (2016) A safety vs efficiency trade-off identified in the hydraulic pathway of grass leaves is decoupled from photosynthesis, stomatal conductance and precipitation. New Phytol 210(1):97–107

Paine CT, Deasey A, Duthie AB (2018) Towards the general mechanistic prediction of community dynamics. Funct Ecol 32:1681–1692

Peuke AD, Rokitta M, Zimmermann U, Schreiber L, Haase A (2001) Simultaneous measurement of water flow velocity and solute transport in xylem and phloem of adult plants of Ricinus communis over a daily time course by nuclear magnetic resonance spectrometry. Plant, Cell Environ 24:491–503

Poorter H, Garnier E (1999) Ecological significance of inherent variation in relative growth rate and its components. Handbook Funct Plant Ecol 20:81–120

Reich PB (2014) The world-wide 'fast-slow' plant economics spectrum: a traits manifesto. J Ecol 102(2):275–301

Ricklefs RE, Latham RE (1992) Intercontinental correlation of geographical ranges suggests stasis in ecological traits of relict genera of temperate perennial herbs. Am Nat 139(6):1305–1321

Rosenberg NJ (1987) Climate of the Great Plains region of the United States. Great Plains Quarterly, 22–32

Sack L, Melcher PJ, Zwieniecki MA, Holbrook NM (2002) The hydraulic conductance of the angiosperm leaf lamina: a comparison of three measurement methods. J Exp Bot 53(378):2177–2184

Schulte PJ, Hinckley TM (1985) A comparison of pressure-volume curve data analysis techniques. J Exp Bot 36(10):1590–1602

Sage RF, Monson RK (1999) C4 plant biology. Academic, New York

Scoffoni C, Rawls M, McKown A, Cochard H, Sack L (2011) Decline of leaf hydraulic conductance with dehydration: relationship to leaf size and venation architecture. Plant Physiol. https://doi.org/10.1104/pp.111.173856

Shipley B, De Bello F, Cornelissen JH, Laliberté E, Laughlin DC, Reich PB (2016) Reinforcing loose foundation stones in trait-based plant ecology. Oecologia 180(4):923–931

Suding KN, Lavorel S, Chapin FS et al (2008) Scaling environmental change through the community-level: a trait-based response-and-effect framework for plants. Glob Change Biol 14(5):1125–1140

Turner NC (1988) Measurement of plant water status by the pressure chamber technique. Irrig Sci 9(4):289–308

Weaver JE (1958) Classification of root systems of forbs of grassland and a consideration of their significance. Ecology 39(3):393–401

Wright IJ, Reich PB, Westoby M et al (2004) The worldwide leaf economics spectrum. Nature 428(6985):821

Zhu SD, Chen YJ, Ye Q et al (2018) Leaf turgor loss point is correlated with drought tolerance and leaf carbon economics traits. Tree Physiol. https://doi.org/10.1093/treephys/tpy013